Evaluation of local pollution sources in the Eurasian Arctic based on integrated data analysis and modeling

Kathy Law, Jean-Daniel Paris, Tatsuo Onishi, Jean-Christope Raut, Louis Marelle, Aurélie Riandet (CNRS-LATMOS and CNRS-LSCE)

Misha Arshinov, Boris Belan, Mikhail Panchenko, D. Chernov (Inst. Atmos. Optics, Tomsk, Russia)

Paris, 26 November 2020

Work Package 4 – Integrating in-situ, satellite and model components for improved environmental assessment

Task 4.3. – Sources and sinks and transport of Arctic pollution determined from an integrated analysis of in-situ and satellite data

Deliverable 4.3.2

Version 002

Introduction

Integrative modelling and data framework

An integrated analysis of existing and new in-situ (surface, lidar), airborne (e.g. YAK) and satellite data (e.g. CALIOP, ADM) is performed based on a case study of oil and gas activities in the Eurasian Arctic, to improve understanding about local sources of anthropogenic pollution such as black carbon and methane (a greenhouse gas and an ozone precursor). Tools such as FLEXPART is used to analyze air mass origins, including pollution plumes, during specific campaign periods as well as the importance of processing such as scavenging by clouds. Combined analysis of airborne and satellite data is used to improve assessment emissions such as those related to resource extraction or domestic combustion in Russia. For example, VIIRS night-light data, combined with analysis YAK data, will provide new information on black carbon emissions from flaring associated with oil/gas production, estimated to be one of the principal sources of BC in the Arctic. Anthropogenic methane source estimation in the Russian Arctic will also benefit from this analysis. Regional model simulations using WRF-Chem combined with analysis of satellite data are used to assess the importance of different sources and to examine pollutant processing.

This work benefits from the model developments on trace gas/aerosol recycling/sources at atmosphere-snow-ice interfaces (Task 2.2).

This work also contributes to the planning for new field campaigns, such as PACES field campaigns investigating pollutant transport from Asia to the Arctic. It aims at laying the foundation for new integrated observational strategy in the detection of changes in emissions of climate forcers and air pollutants.

Methods

Pilot target area: Western Siberia

Siberia is a huge territory, extending over more than 13 million km². For the purposes of this study we focus on the region in northern Siberia where night light satellite data show precisely the fuel and oil exploitations. Fuel exploitations are located where fuzzy halos are observable, due to flaring process. Therefore, the area of study is reduced as indicated in Figure 1 and referred to as “Siberia” in this report.

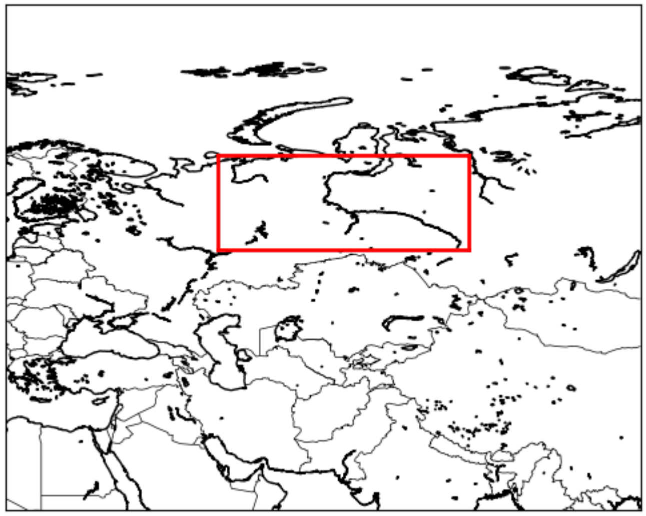

Figure 1. *Map of study area. In red, the inset highlight the western Siberia where most anthropogenic (oil and gas) emissions are located.*

Observations:

a) YAK Aircraft observations

YAK Airborne Extensive Regional Observations in Siberia (AEROSIB) is a series of airborne measurement campaign in Russia as part of a Franco-Russian collaboration with the Institute of Atmospheric Optics (IAO) in order to provide observations of atmospheric gases in Siberia. This study focuses on 2014 and 2017 measurement campaigns, which took place in the Western Siberia. The aircraft used is a Russian aircraft Tupolev. The 2014 measurement campaign is divided into four flights on 15, 16 and 17 October 2014. The route of the aircraft was divided into two loops, one above Kara Sea and the other one above the Ob Gulf, see Table 1 for more details. The 2017 measurement campaign is divided into four flights on 16, 17 and 18 June 16 2017. The aircraft flew a loop from Novosibirsk via the northeast of Siberia, see Table 1 for further details.

Table 1. *Summary of flights of 2014 and 2017 YAK measurement campaigns*

Flight	Date (UTC)	Plateaus (altitude *nb of plateaux)	Cities
Flight 1 (2014)	From October 15 at 3:00 am to October 15 at 5:58 am	8000 meters *3 5000 meters *2 500 meters *2	From Novosibirsk to Salekhard

Flight 2 (2014)	From October 15 at 7:26 am to October 15 at 11:34 am	8000 meters *4 5000 meters *3 500 meters *3	Loop over Kara Sea
Flight 3 (2014)	From October 16 at 4:48 am to October 16 at 9:00 am	8000 meters *3 5000 meters *2 1000 meters *3 500 meters *2	Loop over the Ob River
Flight 4 (2014)	From October 17 at 4:14 am to October 17 at 7:01 am	8000 meters *3 5000 meters *3 1000 meters *1 500 meters *1	From Salekhard to Novosibirsk
Flight 1 (2017)	From June 16 at 4:40 am to June 16 at 6:47 am	4500 meters *1 1000 meters *1 500 meters *1	From Novosibirsk to Surgut
Flight 2 (2017)	From June 16 at 7:48 am to June 16 at 10:53 am	4000 meters *2 500 meters *1	From Surgut to Norilsk
Flight 3 (2017)	From June 17 at 3:03 am to June 17 at 6:22 am	4000 meters *3 500 meters *3	From Norilsk to Surgut
Flight 4 (2017)	From June 18 at 00:07 am to June 18 at 3:39 am	8000 meters *2 4000 meters *2 500 meters *2	Round trip from Novosibirsk to Surgut and back

On the aircraft, carbon dioxide (CO2) and methane are measured with a PICARRO using the CDRS technique. Carbon monoxide (CO) and the ozone (O3) are measured with a Mod. TEI48C and equivalent black carbon (eBC) is measured with an aethalometer *(Panchenko et al., 2015; Paris et al., 2009*).

b) VIIRS satellite data

The VIIRS (Visible Infrared Imaging Radiometer Suite) satellite data provides daily night-light (radiant heat) data (except at during polar day at high latitudes). This has been used by Elvidge et al. (2016) to derive estimates of CO2 emissions from gas flaring using brightness temperatures to distinguish flares.

Model Simulations:

The WRF (Weather Research and Forecasting) and WRF-Chem (WRF with online coupled chemistry) models are used to simulate dynamics and tracers (WRF) and the transport and chemical transformation of trace gases and aerosols simultaneously with the meteorology (WRF-Chem). The model version WRF-Chem ver3.8.1 is used, including updates reported in Marelle et al. (2017) and Marelle et al. (2018) to perform simulations over the Northern Hemisphere with a horizontal resolution of 100km and 50 vertical pressure levels and, at higher resolution over Russia (25 km horizontal resolution. The model was run with SAPRC-99 chemical scheme providing gas-phase tropospheric reactions including VOCs and NOx, coupled MOSAIC and VBS aerosol treatments. Methane concentrations are prescribed. WRF-Chem was run using anthropogenic emissions from ECLIPSEv5 (see next section) and the FINN boreal fire emissions. Boundary and initial meteorological conditions were given by the global NCEP Final Analysis (FNL) and used to nudge the temperature, relative humidity, and winds at every dynamical time-step above the planetary boundary layer. WRF only simulations were also used to drive FLEXPART-WRF particle simulations to investigate the origins of observed pollution plumes over northern Russia.

Methane emission assessment are based on a comparison between in situ measurements and concentrations simulated using the FLEXPART Lagrangian dispersion model version 9.0 (Stohl et al 2005). It uses European Centre for Medium-Range Weather Forecasts (ECMWF) wind fields re-analysis to calculate 10-day backward trajectories. To produce spatial steady outputs independent from speed which can vary between landing, take-off and plateau phases, releases are chosen every 0.15° of latitude or longitude or 100 meters following altitude folllowing Paris et al. (2010). Results are produced on a 1°x1° grid.

Pollutant emission inventories:

ECLIPSE: Model runs investigating source contributions to Arctic BC were carried out using the ECLIPSE anthropogenic emissions, available at 50km resolution (*Klimont et al., 2017*). These emissions included improved estimates for emissions from Russian gas flaring and seasonality of domestic (wood) combustion (*Stohl et al. 2015*). Further details on the sectors are given below.

Arctic Black Carbon (ABC): Higher resolution BC emissions (10km) from *Huang et al. (2015)* were also used for BC tracer runs investigating origins of pollutant (BC) plumes observed during the YAK-AEROSIB aircraft flights in October 2014.

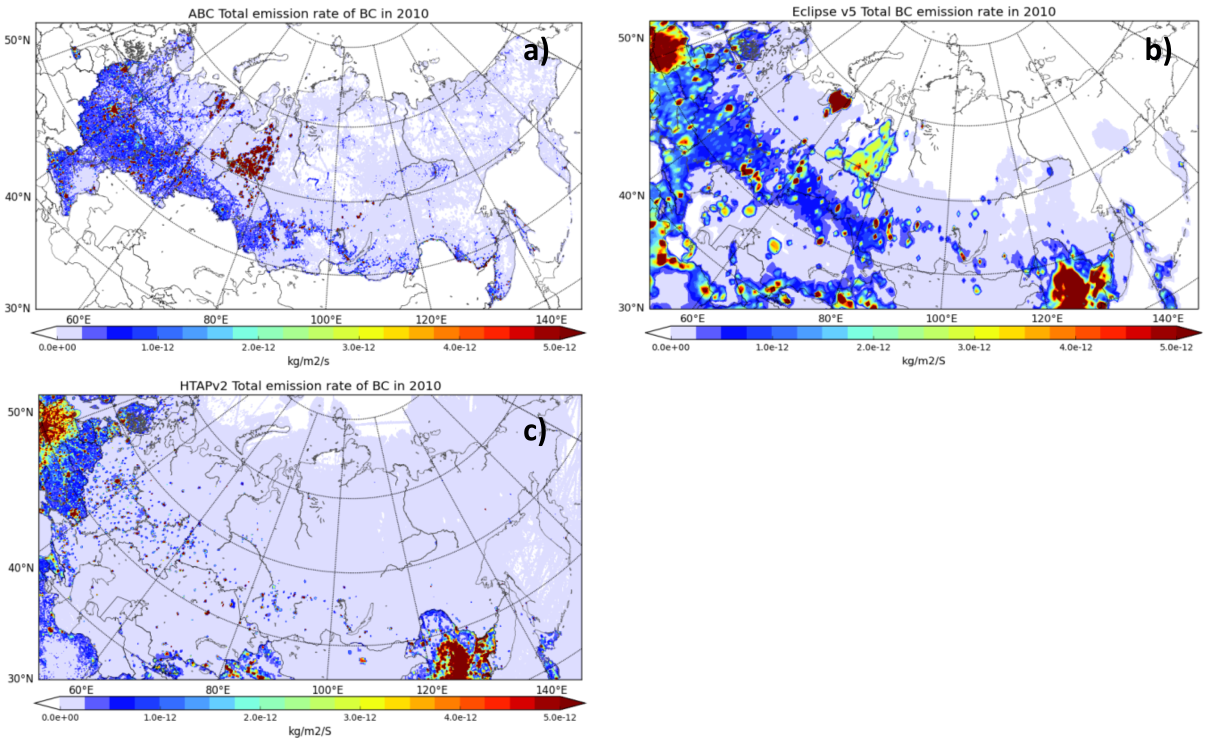

Figure 2*: Comparison of different emission inventories. BC emissions from* ***(a)*** *the Arctic Black Carbon dataset (ABC, Huang et al., 2015),* ***(b)*** *ECLIPSEv5 (Stohl et al., 2015), and* ***(c)*** *HTAPv2 (Janssens-Maenhout et al., 2015) for the year 2010 (From Sergent, 2017; Schmale et al., 2018).*

Figure 2 illustrates the differences between BC emission inventories over Russia for 2010. The Arctic Black Carbon (ABC) emissions have higher BC emissions from flaring, residential and industrial sectors (224kT/yr) than and ECLIPSEv5 (170kT/yr) ECLIPSEv5 (*Klimont et al., 2016*). Differences can be seen in the ECLIPSE and ABC emissions from the flaring sector over the Ob valley region in north-west Siberia. Differences in emissions linked to oil and gas extraction activities are investigated below. They have already been shown to be a significant source of BC in the Arctic (*Stohl et al., 2013*), but large uncertainties exist in these emissions. It can also be noted that the HTAPv2 has no emissions from this sector.

Methane emission inventories:

Two methane anthropogenic inventories and one methane natural inventory are used in this study. EDGAR inventory includes 21 anthropogenic sectors. We gather them into 6 main sectors: energy, domestic, industry, transportation, agriculture and waste (see Table 2 for activities involved into each category). EDGAR inventory is available as grids with a resolution of 0.1°x0.1°.

Table 2: *Main sectors and EDGAR activities involved in each sector*

Main sector	Activities involved
Energy	Power industry, fuel exploitation, fossil fuel fire
Domestic	Energy for building
Industry	Combustion for manufacturing
Transportation	Road transportation
Agriculture	Agriculture waste burning, manure management, enteric fermentation, agricultural soils
Waste	Solid waste landfills, waste water handling, solid waste incineration

The second anthropogenic methane inventory is the Evaluating the Climate and Air Quality Impacts of short-Lived Pollutants (ECLIPSE) inventory~~.~~ It includes 6 anthropogenic sectors (Energy, Domestic, Industry, Transportation, Agriculture, Waste), as grids with a resolution of 1°x1°.

Natural biogenic emissions of methane in Siberia are simulated using two different models. The one dedicated to wetlands emissions is the Organizing Carbon and Hydrology In Dynamic Ecosystems (ORCHIDEE) inventory from the Institut Pierre Simon Laplace (IPSL). It provides methane emissions from wetlands, gridded at 1°x1°. The inventory dedicated to the emissions of methane from forest fires is GFED (Global Fire Emissions Database), gridded at 0.25°x0.25°.

Results and Discussion

1. Contributions of local and remote sources to Arctic SLCFs:

The WRF-Chem model was run at 100km using ECLIPSEv5a emissions for spring and summer 2012 and 2050 to examine local and remote sources contributing to aerosol and ozone distributions and to estimate their radiative effects (*Marelle et al. 2018*). The simulation was performed on a polar stereographic projection with a horizontal resolution of 100km and 50 vertical hybrid terrain-following vertical pressure levels using hydrostatic pressure. The model was run with SAPRC-99 chemical scheme providing gas-phase tropospheric reactions including VOCs and NOx, coupled MOSAIC and VBS aerosol treatments. Methane concentrations are prescribed. Boundary and initial meteorological conditions were given by the global NCEP Final Analysis (FNL) and used to nudge the temperature, relative humidity, and winds at every dynamical time-step above the planetary boundary layer.

The results show important contributions from black carbon flaring emissions over northern Russia which are transported over the Arctic Ocean (see Fig. 3) in spring and which contribute up to 60% to surface deposition of black carbon over the Arctic.

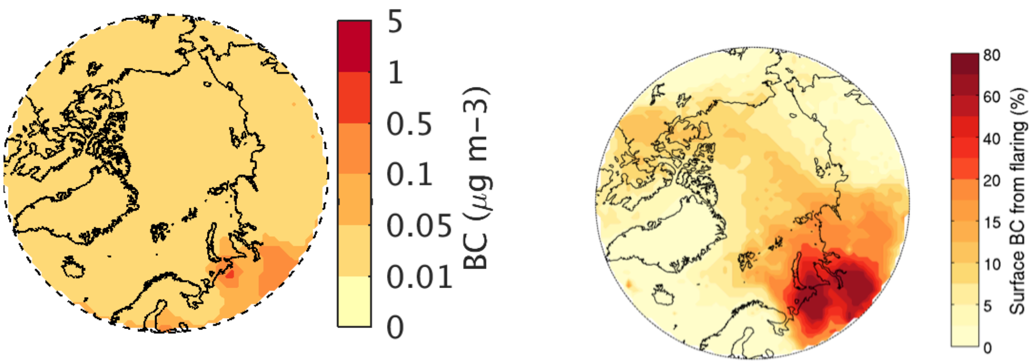

Figure 3: *Modelled black carbon distributions in spring 2012 (left) and % contribution to surface black carbon from gas flaring emissions (right panel).*

Simulations with and without Arctic shipping emissions showed significant increases in Arctic surface ozone with implications for future regional air quality. Quantification of future radiative effects estimated important indirect effects from Arctic shipping of the same magnitude as remote anthropogenic and boreal fire emissions due to the direct emission of shipping emissions into the cloudy Arctic boundary layer.

2. Source estimations

a) Black Carbon: Focus on Russian oil and gas sector

A combined analysis of YAK aircraft data, VIIRS satellite data and modelling has been used to investigate discrepancies in black carbon emissions from oil and gas extraction activities in northern Siberia. A YAK aircraft campaign took place in October 2014 with flights over the Ob valley region as shown in Figure 4. The flights surveyed the troposphere between the boundary layer (< 1km) and 8km. Analysis of equivalent black carbon (EBC) measurements together with trace gas measurements of CO, CO2 and CH4 was used to identify pollution plumes with characteristics specific to emissions from the oil/gas flaring sector: elevated BC, CO2 but not CH4 which is characteristic of gas venting rather than flaring. Identified plumes along the flights are shown in Figure 5 where measured EBC enhancements of up to 0.2-0.3 μg m^{-3} were observed in the boundary layer. Results from a WRF-Chem simulation run at 25km with ECLIPSEv5 emissions are also shown. The model is able to capture some of the plumes but not all of them. This could be due to model dynamics, chemical processing or emissions. Here, we focus on examining the emissions as a source of these differences.

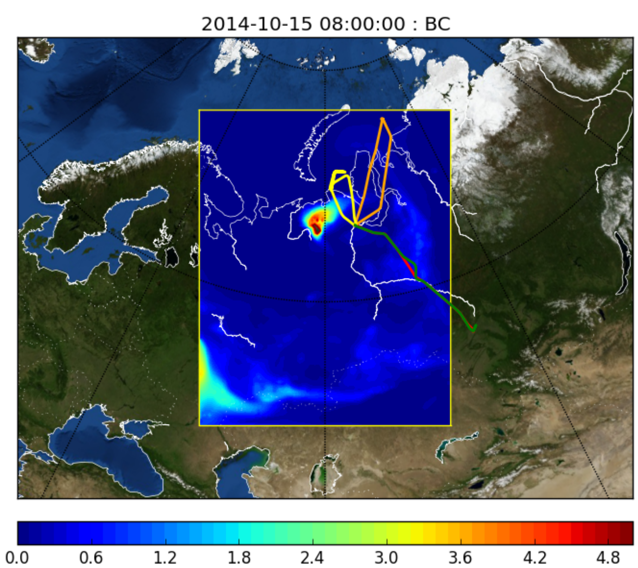

Figure 4: *Flight tracks for the YAK aircraft campaign in October 2014: Flight 1 (15 October, green), Flight 2 (16 October, yellow), Fight 3 (16 October, orange), and Flight 4 (17 October, red) superimposed on simulated black carbon concentrations (micro g/cm-3) for 15 October 2014.*

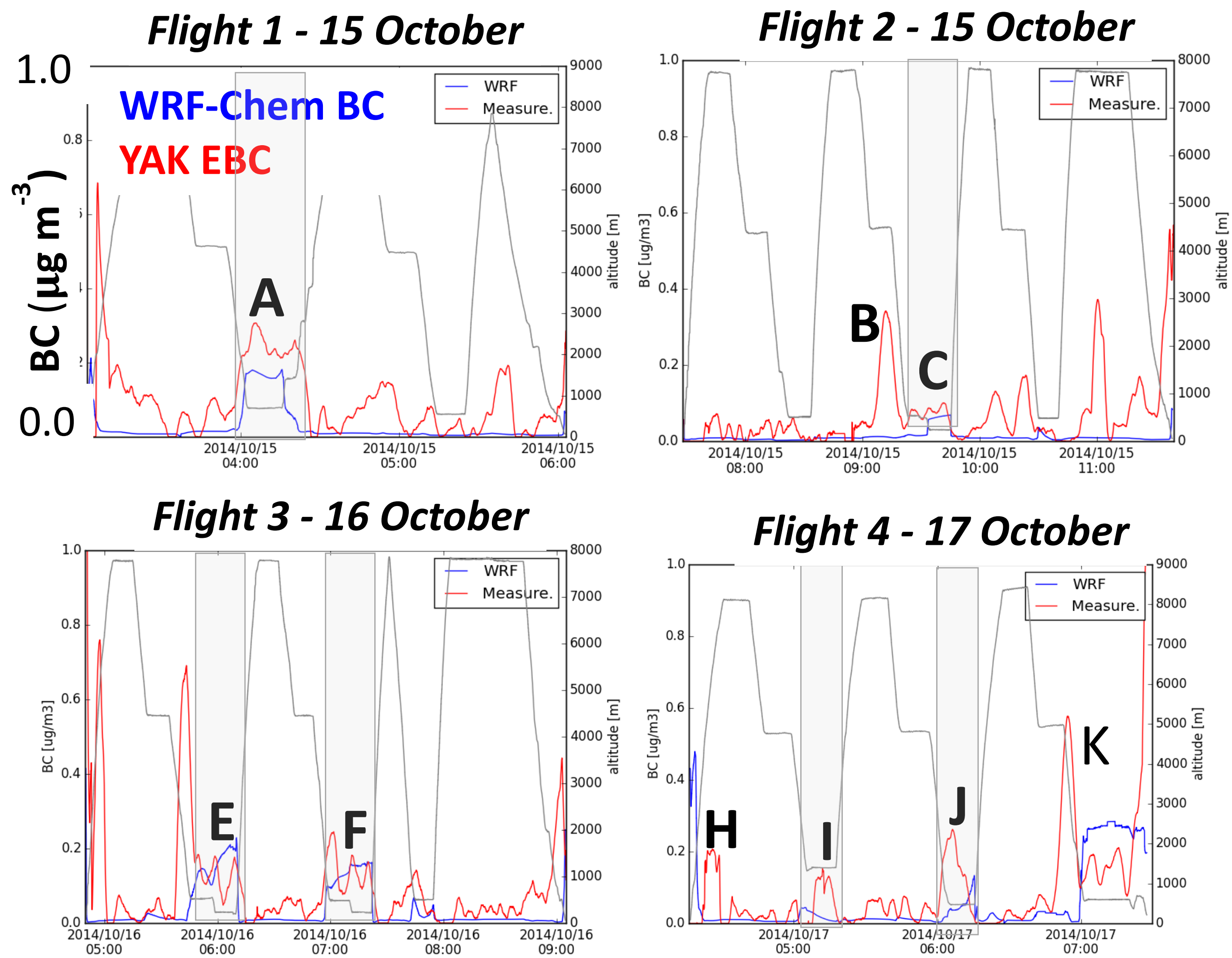

Figure 5: *Observed equivalent black carbon and simulated BC along the YAK flight tracks. Plumes identified as originating from oil/gas emissions are denoted by the letters (see text for details).*

To examine reasons for the discrepancies between observed and simulated WRF-Chem BC and to understand differences between the ECLIPSE and ABC emissions, FLEXPART-WRF was run backwards from the identified plumes using output from a WRF simulation (9-17 October 2014 at 5 km resolution) and mapped onto the emission footprints. In cases of plumes (C, E and F) that are captured well by WRF-Chem, the FLEXPART-WRF emission footprints show a higher contribution from ECLIPSE emissions compared to ABC which are much lower. In the case of Plume F, this plume originates from Nenets-Yamal in the north-west of the region. In contrast, WRF-Chem underestimates plumes A and J originating from the Khantys-Mansis region. In this case, the FLEXPART-WRF footprints show a much stronger flaring signature using the ABC emissions and too low a contribution using ECLIPSE. In plume I which is not captured in the WRF-Chem simulation, neither emission dataset has a footprint suggesting that emissions are missing over the region south of Nenets-Yamal (or that this plume has other origins).

A preliminary investigation was also carried out to investigate the possible influence of daily variability in the flaring emissions using VIIRS nightlight data. FLEXPART-WRF forward simulations were run from 9-17 October from VIIRS nightlights and initialised with either constant BC emissions (ABC Huang (regional annual mean) emissions weighted by number of VIIRS 2014 flares (red spots) in 1 x 1 deg. grid) or daily varying emissions (ABC Huang emissions only on days when VIIRS flares reported). One caveat is that clouds may mask flares. Simulated BC tracer along the flight tracks provides an estimate of the maximum contribution since no chemical processing or deposition is taken into account. Nevertheless, differences of up to a factor of 3 are found between the runs with constant emissions versus the runs with daily varying emissions.

In summary, the YAK aircraft data showed clear enhancements in EBC due to flaring over northern Russia. The analysis shows that discrepancies between the modelled and observed BC can be partly explained by inconsistencies in ECLIPSEv5 emissions (compared to ABC) or missing emissions. The results suggest that Russian flaring emissions could be higher, i.e. a combination of ECLIPSE and ABC plus the missing emissions and that it is important to take into account daily variability in flaring emissions. The latter is the subject of on-going work.

b) Methane:

Comparison of 'prior' methane inventories

All sectors gathered the estimated emissions by ECLIPSE are higher than the emissions estimated by EDGAR, respectively equal to 346800 kt/year and 335800 kt/year. Looking at the 6 selected sectors (Figure 6), both inventories show relatively high anthropogenic methane emissions in the energy, agriculture and waste management sectors. On a global scale, the energy sector, the one of interest in this study, already shows a significant difference between the two inventories, ECLIPSE being superior to EDGAR by a factor of 1.5.

Figure also shows natural emissions on a global scale. Wetland emissions are shown in orange, for the 2014 campaign (referred to as "wetlands (Oct)") and the 2017 campaign (referred to as "wetlands (Jun)"). The magnitude of these emissions is 143200 kt/year and 177300 kt/year respectively for the 2014 and 2017 measurement campaigns. Forest fires are also shown in ***Figure*** in red, for the 2014 measurement campaign (indicated by "Forest fires (Oct)") and the 2017 measurement campaign (indicated by "Forest fires (Jun)"). The magnitude of these emissions is 22800 kt/year and 10600 kt/year respectively for the 2017 and 2014 measurement campaigns.

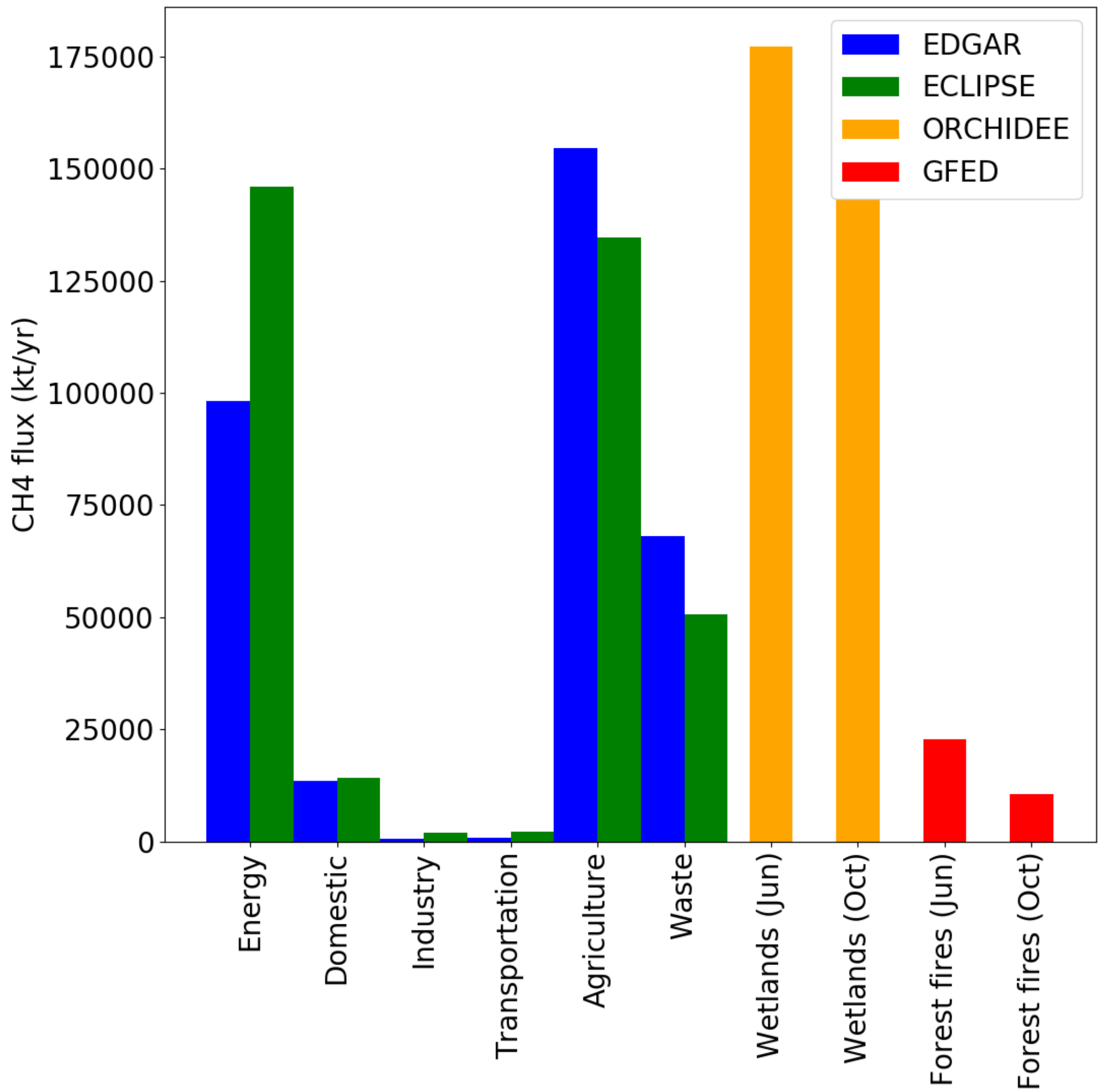

Figure 6: *Global anthropogenic methane emissions for the six sectors. Blue is the anthropogenic inventory EDGAR, green is the anthropogenic inventory ECLIPSE, red is emissions due to forest fires and the natural emissions from wetlands are in orange.*

As the study is mainly focused on Siberia, a closer look is now given to anthropogenic emissions in this region (see Fig. 6). The energy sector is clearly the largest anthropogenic emitting sector in the study area, however there is a large difference in estimate between the two inventories, ECLIPSE estimates methane emissions in this sector at about 14400 kt/year while EDGAR estimates methane emissions at about 2700 kt/year, so ECLIPSE is about 5.3 larger than EDGAR.

Wetlands are also an important source of methane in the region, both in June 2017 (about 33400 kt/year) and in October 2014 (about 7800 kt/year). The difference in magnitude between the two years is mainly due to the seasonal variability of methane emissions from wetlands. Indeed, this methane is released into the atmosphere by methanogenic bacteria that decompose organic matter. In summer, there are more plants than in winter, and therefore more emissions. Although it is important to look at the methane emissions caused by fires, the two years studied here do not show significant emissions from these sources during the measurement campaigns that we analyze in this report. Subsequently, this source will no longer be considered.

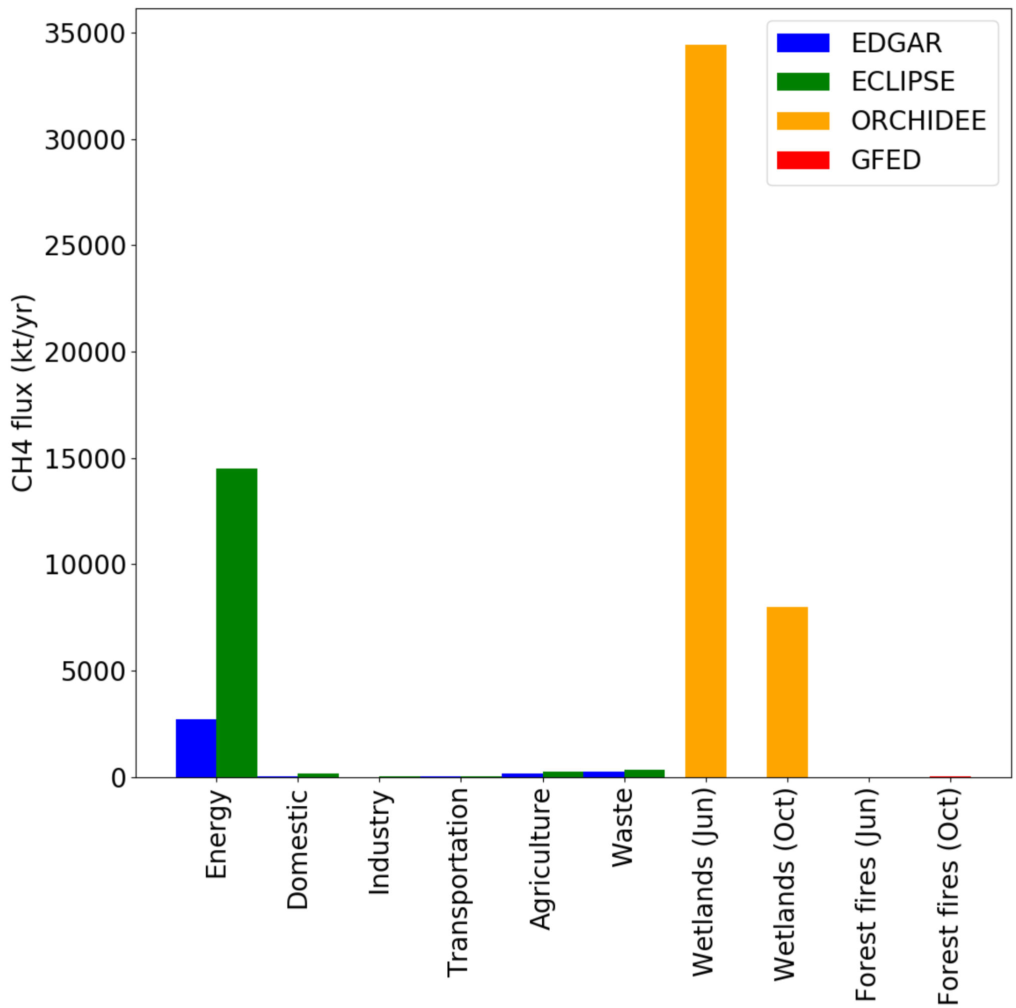

***Figure** 7: anthropogenic methane emissions for the six sectors in Siberia. Blue is the anthropogenic inventory EDGAR, green is the anthropogenic inventory ECLIPSE, red is emissions due to forest fires and the natural emissions from wetlands are in orange.*

The methane measured during the campaigns have been simulated using the two inventories for anthropogenic sources (including anthropogenic fossil fuel and non-fossil-fuel), also accounting for natural sources (wetlands and forest fires). The result for the first flight of the 2017 campaign is presented in Fig. 8 below.

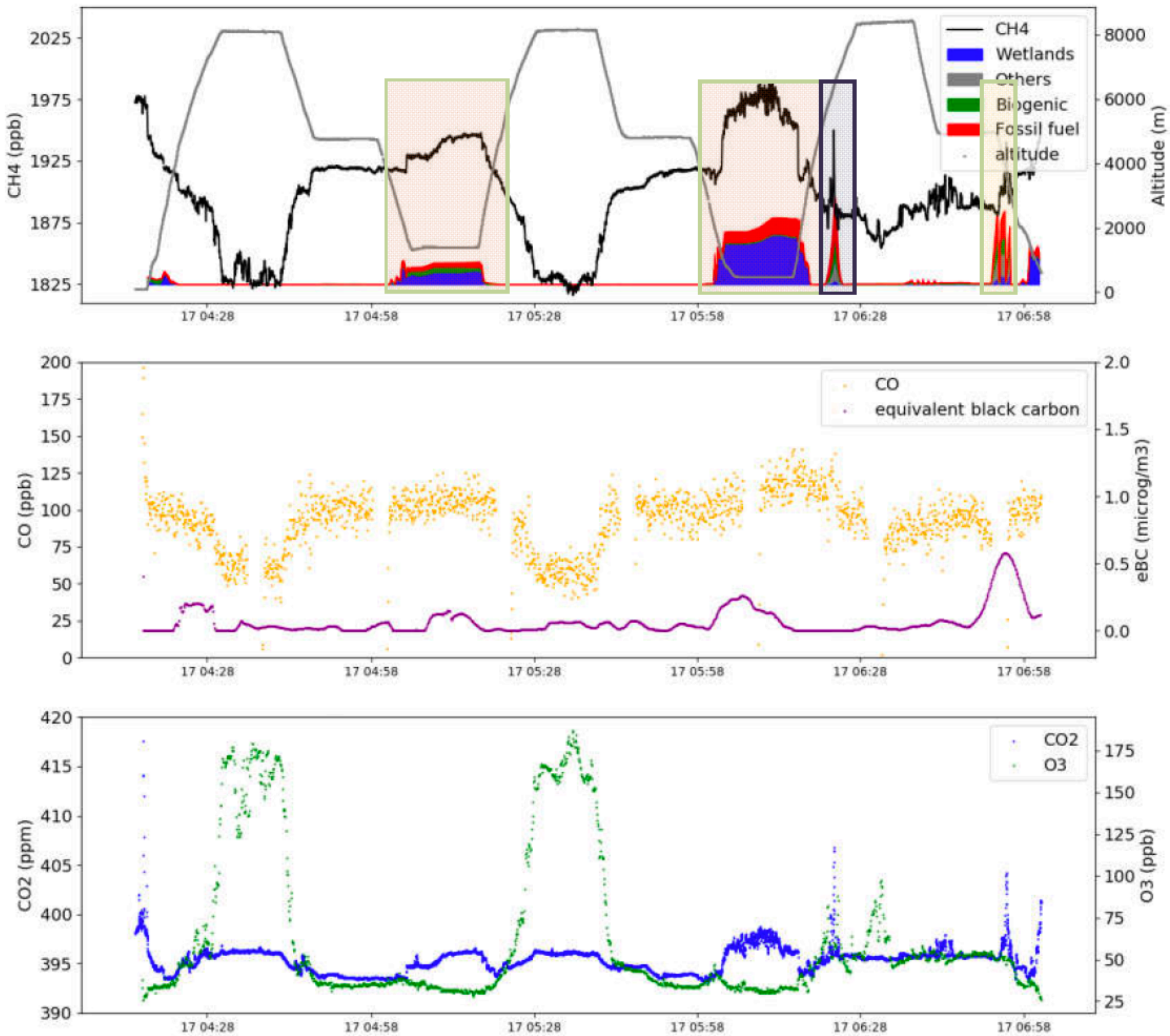

Figure 8. *Measured and simulated methane as well as other key species measured in situ during the first flight of the YAK-AEROSIB 2017 campaign.*

The FLEXPART simulation only estimates the contribution of CH4 enrichment of air masses over the last 10 days, therefore the absolute concentration is not accurately simulated (an arbitrary offset is applied for the figure). Rather, the excess CH4 due to regional influences is comparable to variability in the observed signal. In Fig. 8 top panel, methane enhancements when the aircraft flies at low altitude (typically in the boundary layer) is simulated as coming from a combination of wetland and fossil fuel sources. On the opposite, in the free troposphere, the simulation indicates no significant contribution from regional sources to methane variability. Low altitude enhancements attributed to simulated sources can reach a few tens of ppb, matching the observed enhancements at the lowest flight segments.

Here, the aim is to estimate to what extent methane emissions in Western Siberia are compatible with the inventories available. We calculate compatible values for emissions as per the following steps:

1) Calculation of theoretical excesses of methane emitted for each sector ($\Delta CH4_{inventory*FLEXPART}$). To do so, FLEXPART footprints are multiplied by each inventory, assuming that variations of methane mixing ratios are only due to emissions from the ground and that thus there is no chemical process involved. A conversion is made to obtain part-per-million (ppb). FLEXPART is given in m^{-1}, as explained in Seibert and Frank (2004).
2) Calculation of practical excesses of methane associated to fuel and gas exploitation ($\Delta CH4_{obs}$). Episodes are isolated from the whole measurement campaign. An episode is defined as a period which significant air mass comes from the area of study and showing relatively high methane mixing ratio. An episode can hypothetically be divided into a background, a methane excess due to natural sources and the excess of methane related to fuel and gas exploitation. The background, estimated as the mixing ratio measured in the free troposphere before the episode, is subtracted to the methane mixing ratio such as the methane excess from natural sources calculated previously.
3) Calculation of methane emissions in the area of study from fuel and gas exploitation sector. Linear relationship between excess of methane calculated and methane emissions is supposed, which gives the relation used to calculate methane emissions by observations:

$$E_{YAK} = E_{inventory} * \frac{\Delta CH4_{obs}}{\Delta CH4_{inventory*FLEXPART}}$$

With E_{YAK} as the methane emissions estimated by calculations, $E_{inventory}$ as the methane emissions given by a considered inventory.

Results are shown if Fig. 9. While the two inventories differ from each other by a factor 7 on “Energy” source intensity, and disagree strongly on the spatial distribution of fluxes (not shown), we find that a mean value of 5,6±3,4Mt CH4 y^{-1} can reconcile the two inventories in compatibility with the observed measurements at the lowest altitudes.

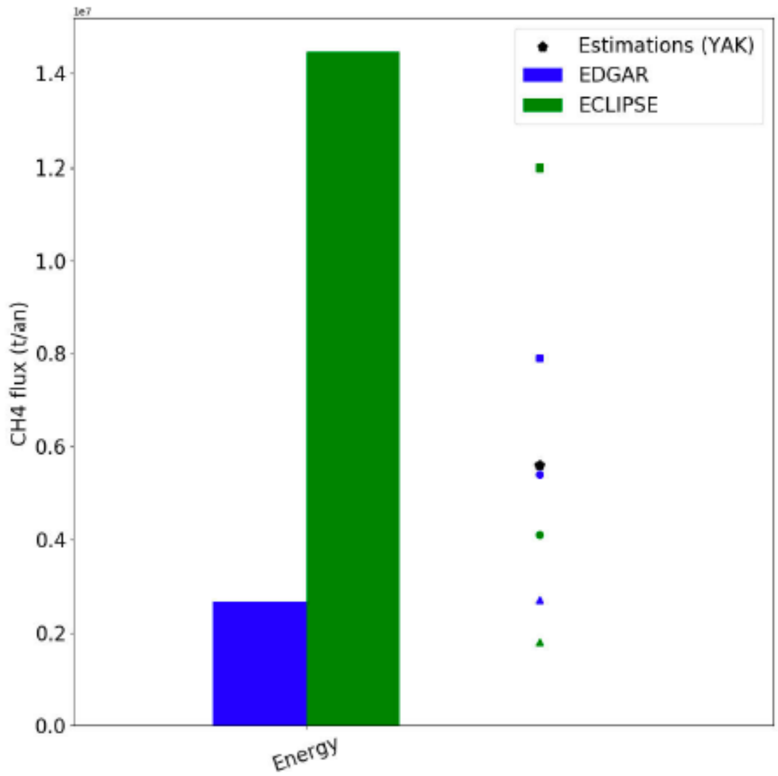

Figure 9. *CH4 fluxes for Energy in western Siberia according to the two inventories, and the values compatible with our observations (one dot corresponds to one flight segment in and out of the boundary layer, with sufficient sensitivity to the regional anthropogenic emissions).*

3. Conclusions:

The results presented here show the benefit of combined approaches combining the analysis of airborne, satellite data together with modelling to better understand deficiencies in emission inventories of short-lived climate forcers: black carbon and methane. Such "ground-truthing" using observations and models are needed in order to reduce uncertainties in model predictions.

References

Caseiro, A., Gehrke, B., Rücker, G., Leimbach, D., and Kaiser, J. W.: Gas flaring activity and black carbon emissions in 2017 derived from Sentinel-3A SLSTR, Earth Syst. Sci. Data Discuss., https://doi.org/10.5194/essd-2019-99, in review, 2019.

Huang, K., Fu, J. S., Prikhodko, V. Y., Storey, J. M., Romanov, A., Hodson, E. L., et al. (2015). Russian anthropogenic black carbon: Emission reconstruction and Arctic black carbon simulation. *Journal of Geophysical Research: Atmospheres*, 2015JD023358. http://dx.doi.org/10.1002/2015JD023358

Elvidge, C.D.; Zhizhin, M.; Baugh, K.; Hsu, F.-C.; Ghosh, T. Methods for Global Survey of Natural Gas Flaring from Visible Infrared Imaging Radiometer Suite Data. Energies 2016, 9, 14.

Janssens-Maenhout, G., Crippa, M., Guizzardi, D., Dentener, F., Muntean, M., Pouliot, G., et al. (2015). HTAP_v2.2: a mosaic of regional and global emission grid maps for 2008 and 2010 to study hemispheric transport of air pollution. *Atmospheric Chemistry and Physics, 15*(19), 11411-11432. https://www.atmos-chem-phys.net/15/11411/2015/

Klimont, Z., Kupiainen, K., Heyes, C., Purohit, P., Cofala, J., Rafaj, P., et al. (2017). Global anthropogenic emissions of particulate matter including black carbon. *Atmospheric Chemistry and Physics, 17*(14), 8681-8723. https://www.atmos-chem-phys.net/17/8681/2017/

Marelle, L., J.-C. Raut, K. S. Law and O. Duclaux, Current and Future Arctic Aerosols and Ozone From Remote Emissions and Emerging Local Sources—Modeled Source Contributions and Radiative Effects, Journal of Geophysical Research : Atmospheres 123.22, p. 12-942, 2018.

Marelle, L., J.-C. Raut, K. S. Law, L. K. Berg, J. D. Fast, R. C. Easter, M. Shrivastava and J. L. Thomas, Improvements to the WRF-Chem 3.5. 1 model for quasi-hemispheric simulations of aerosols and ozone in the Arctic ». In : Geoscientific Model Development 10.10, p. 3661-3677, 2017

Paris, J.-D., Stohl, A., Ciais, P., Nédélec, P., Belan, B. D., Arshinov, M. Yu., and Ramonet, M.: Source-receptor relationships for airborne measurements of CO2, CO and O3 above Siberia: a cluster-based approach, Atmos. Chem. Phys., 10, 1671–1687, https://doi.org/10.5194/acp-10-1671-2010, 2010.

Schmale, J., Arnold, S. R., Law, K. S., Thorp, T., Anenberg, S., Simpson, W. R., Mao, J., and Pratt, K. A.: Local Arctic air pollution: a neglected but serious problem, Earths Future, 6, 1385–1412, https://doi.org/10.1029/2018ef000952, 2018.

Sergent, N., Uncertainties in black carbon emissions in the Russian Arctic, Master thesis, Université de Versailles et Saint-Quentin en Yvelines, France, 2017.

Stohl, A., Klimont, Z., Eckhardt, S., Kupiainen, K., Shevchenko, V. P., Kopeikin, V. M., & Novigatsky, A. N. (2013). Black carbon in the Arctic: the underestimated role of gas flaring and residential combustion emissions. *Atmospheric Chemistry and Physics, 13*(17), 8833-8855. http://www.atmos-chem-phys.net/13/8833/2013/

Stohl, A., C. Forster, A. Frank, P. Seibert, G. Wotawa. Technical note: The Lagrangian particle dispersion model FLEXPART version 6.2. Atmospheric Chemistry and Physics Discussions, European Geosciences Union, 2005, 5 (4), pp.4739-4799.